V European Conference on Computational Fluid Dynamics
ECCOMAS CFD 2010
J. C. F. Pereira and A. Sequeira (Eds)
Lisbon, Portugal, 14–17 June 2010

ISLAND WAKE ASYMMETRIES: FROM LABORATORY TO NUMERICAL MODELISATION

A. Stegner[*], R. Caldeira[†], and C. Dong[††]

[*]Laboratoire de Météorologie Dynamique (LMD)
Ecole Polytechnique, Palaiseau 91128, France
e-mail: stegner@lmd.ens.fr

[†] Center of Marine and Environmental Research (CIIMAR)
Portugal
rcaldeira@ciimar.up.pt

[††]Institute of Geophysics and Planetary Physics (IGPP)
University of California, Los Angeles, CA 90095-1565
cdong@atmos.ucla.edu

Key words: Cyclones, anticyclones, instabilities, island wakes, physical oceanography

Abstract.*Island wakes are regions of strong eddy activity impacting the retention and transport of organic matter, and subsequent biological enrichment. Various asymmetry of theses eddies were studied by means of laboratory experiments and numerical simulations. At large scale, the linear stability analysis of frontal wake flows explain the preferred formation of anticyclonic vortices in the lee of large islands. Once they are formed, theses large-scale anticyclones tend to be more stable and robust to external strain perturbations than their cyclonic counterparts. Hence, if the island or the archipelago is large enough (larger than the deformation radius) we could expect the predominance of large anticyclones in the oceanic wake. Moreover, in such case, a transition from absolute to convective instability was also found for rotating shallow-water wakes. The patterns of the convectively unstable wake strongly differ from the standard two-dimensional Karman street and the vortices are shed at an higher frequency. However, not only the size but also the coastal shape of the island could have a strong influence on the meso-scale eddy formation. For instance, the topography of the Madeira Archipelago favors the formation of cyclonic eddies in agreement with recent remote sensing and in-situ observations. At smaller scales, ageostrophic filaments, wind forcing and ageostrophic instabilities controls the dynamics. Recent experimental and numerical results have shown that an island wake flow may exhibit a transient and three-dimensional instability in the region of intense anticyclonic vorticity. This instability is a branch of the inertial (or centrifugal) instability in the framework of rotating, stratified shallow-water flows. Considering the small vertical wavelenght selection (10-50 m for a standard thermocline), this instability can hardly be captured by regional circulation models having a low vertical resolution.*

1 INTRODUCTION

The role of oceanic islands wakes in the biological enrichment and the retention of surface pollutants is an area of growing interest. The geostrophic balance of cyclonic eddies induce a vertical advection of the deep chlorophyll maxima or the enhancement of biological productivity due to the deep nutrient upwelling [1, 2]. On the other hand, large-scale and long lived anticyclonic vortices in the island wake create transport barriers and core trapping [3] which could lead to an incomplete horizontal mixing. Such large anticyclonic structures promote downwelling in their core and low nutrient concentration in the euphotic layer [4]. Besides, cyclogeostrophic anticyclones may be the source of three-dimensional inertial instabilities on the vortex edge. Such ageostrophic instability enhance the horizontal transport and the vertical mixing of passive tracers in the island wake [5, 6]. Motivated by this oceanographic context, laboratory and numerical experiments were carried out to study the impact of the island size, the flow intensity and the stratification on the asymmetry between cyclonic and anticyclonic vortices formed in the island wake.

In-situ measurements and general circulation models have shown that large-scale vortices, i.e. eddies whose characteristic radius is larger than the local deformation radius, are ubiquitous in the oceans. A striking characteristic of these large-scale and long-lived structures is that anticyclonic vortices tend to be more prevalent than cyclonic ones. Large-scale anticyclones are frequently observed in the lee of oceanic archipelago such as Hawaii [7, 8] or the Canaria [3]. According to several numerical studies [9, 10, 11] large-scale flows increase the stability of anticyclonic structures compared to their cyclonic counterpart. Cyclones tend to be more distorted and unstable when their size exceeds the deformation radius. However, very few studies investigate this specific asymmetry, which occurs when the isopycnal deviations become finite, for large oceanic island. In such a case, both the global flow (the wake) and local structure (the vortices) structures could be affected.

For small islands interacting with a strong current the inertial instabilities may strongly destabilize the detached shear layers [12, 13] in the near wake and anticyclonic eddies in the vortex wake [14,15,16]. Indeed, three dimensional perturbations growth in a localized region, at the edge of the anticyclonic vortices, if the dimensionless vorticity within the vortex $\xi/f<-1$ is negative enough, where ξ is the relative vorticity and $f=2\Omega_0$ the Coriolis parameter. For a columnar vortex, the vertical wavelength of the most unstable modes is mainly controlled by the dimensionless vorticity, the Reynolds number and the relative stratification parameter N/f [17]. If the incoming oceanic flow is strong enough or if the island diameter is too small the eddies formed in the wake will reach large vorticity values. In such case, the selective destabilization of anticyclonic shear and eddies, will favor the emergence of coherent cyclones in the oceanic island wake.

Another source of asymmetry between opposite sign eddies in the wake could be due to the island shape itself even for a pure two-dimensional flow which is not affected by the rotation and the stratification. For an asymmetrical island the detached boundary layers of the near wake may differ in width and amplitude. In such case, the vortices, which are formed further down in the wake, may differ in size (radius) and intensity (core vorticity).

We present here a short review of our recent experimental and numerical studies on island wake dynamics in the deep ocean. We identify, for a rotating and stratified surface layer, the main dimensionless parameters who control the wake asymmetries. We analyse the various dynamical processes at large or small scale which may favor the predominance of cyclonic or anticyclonic eddies beyond oceanic islands.

2 ISLAND WAKE CONFIGURATION AND DYNAMICAL PARAMETERS

2.1 Deep oceanic island configurations

For an island wake in deep water, when an upper surface current encounter an isolated island or an archipelago, the boundary stress associated with the nearshore or the lateral side of the island induce a strong boundary shear flow. In this deep water case the influence of bottom drag becomes negligible, as discussed by Tomczak [18]. In a first approximation we consider, for a deep ocean wake, that the motion has a strong baroclinic component with intense velocities in the surface layer while the deep lower layer remains almost at rest. The free surface deformation is then neglected in comparison with the internal isopycnal deviations. The wake dynamic will be mainly controlled by the surface current velocity V, it's characteristic thickness h, the mean island diameter D and the horizontal dissipation (i.e. the horizontal turbulent viscosity).

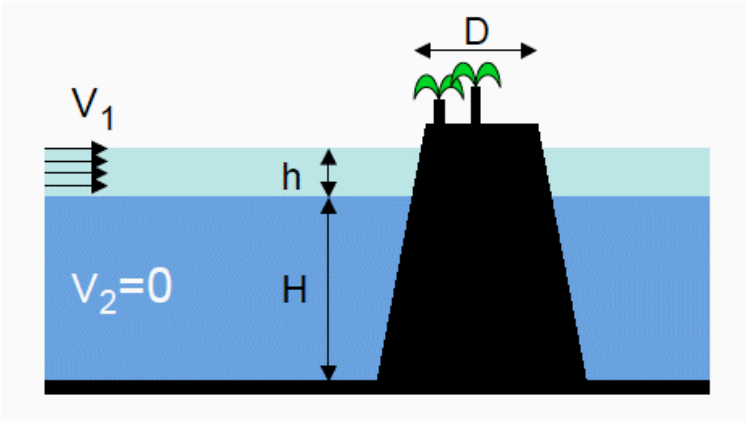

Figure 1: Geometrical configuration of an idealized island in the deep ocean interacting with a surface current.

2.2 Rotation and stratification

In order to quantify the impact of the rotation we generally use the island Rossby number Ro = V/(R*f*) where *V* is the characteristic current velocity and R the typical island radius. However, a more accurate description of the vortex dynamics in the wake will be given by the vortex Rossby number $(Ro)_e = V_e/(R_e f)$, where R_e and V_e are the typical eddy radius and velocity or the relative core eddy vorticity $\varepsilon=\xi/f$ where ξ is the maximum core vorticity. If the island and the eddy Rossby number have generally the same order of magnitude, the local core eddy vorticity may be much larger than a global Rossby number, see figure X for instance.

An other parameter which governs the island wake dynamics is the Burger number $Bu=(R_d/R)^2$, this latter is given by the relative island size. Small (large) island in comparison with the local deformation radius R_d leads to large (small) Burger number. The deformation radius takes into account the combined effect of the rotation and the vertical stratification of the upper thermocline. For an idealized two layer stratification the baroclinic deformation radius could be approximated by $R_d^2 \sim g^* h/f^2$ (with the reduced gravity $g^*=(\Delta\rho/\rho)g$) when the upper thermocline $h \ll H$ is much thinner than the deep oceanic layer H. For a linearly stratified thermocline the deformation radius of the first baroclinic mode is given by $R_d=Nh/f=Sh$ where N is the typical Brunt-Vaisala frequency of the upper layer and $S=N/f$ the stratification parameter. In the mid-latitude

oceans, typical deformation radius are in between 15 km to 60 km. Hence, many oceanic wakes correspond to a large-scale flow configuration (Bu <<1) leading to finite isopycnal deviations. In such case, the vortex street could strongly differ from the classical Kármán wake.

2.3 Dissipation

The vertical diffusion of momentum is controlled by the Ekman $Ek=\nu_v/fh^2$ number while we usually use the Reynolds $Re=VD/\nu_h$ number to quantify the horizontal dissipation in the wake flow. The oceanic stratification induces a significant discrepancy between the horizontal ν_h and the vertical ν_v turbulent viscosity and the Ekman and Reynold numbers are therefore two independent parameters.

2.4 Shallow-water constrain

An important parameter for deep island wake is the vertical aspect ratio a= h/R where h is the upper surface current thickness (i.e. the thermocline depth) and R the typical horizontal scale of the island or the eddies. Note that h = 100–200m is generally much smaller than the total water depth H =1–2km for isolated volcanic islands in the deep ocean. This aspect ratio parameter is very small a ~ 0.01 in the ocean and we could therefore expect an hydrostatic wake flow.

3 LARGE-SCALE WAKES

3.1 The frontal regime

Depending on the value of the Burger number, one distinguishes various dynamical regimes for small island or vortex Rossby number. The classical quasigeostrophic model is defined when Bu=*O(1)*. In that limit, cyclones and anticyclones obey the same equation. The second regime corresponds to the frontal regime and is defined by Bu=*O*(Ro)<<1. In this regime, the flow is expected to follow at leading order the frontal geostrophic asymptotic model [19]. In that model, the isopycnal deviations are order unity and the evolution of cyclonic and anticyclonic structures should differ strongly. This dynamical regime apply for large scale island when the mean island radius is two or three times larger than the local deformation radius.

3.2 Experimental configuration

To reproduce in laboratory the dynamic of a surface current interacting with an isolated and steep island (Figure. 1) we used a two-layer salt stratification and we towed in the upper layer a cylinder of diameter D and height h (Figure. 2). We assume that the motion of the cylinder transfer momentum mainly in the upper layer and that the dynamic is then governed by the first baroclinic mode $R_d^2=g*h/f^2$. This will be generally the case for a deep lower layer, namely when h << H. The cylinder diameter may then be equal to or larger than the deformation radius R_d and this experimental setup allows us to study the dynamics of quasigeostrophic and large-scale wakes [20].

Standard particle image velocimetry PIV was used to measure the horizontal velocity field. Small buoyant particles were put in the upper layer and lightened with a horizontal laser sheet of wavelength 670 nm. The fluctuations of the internal interface between the upper and the lower layer are measured using a laser-induced fluorescence LIF technique. The fluorescent dye (Rhodamine 6G), put in the upper layer, was illuminated by a vertical laser sheet. Hence, the fluorescent upper layer appeared bright while the deep lower layer, transparent to the laser sheet, remained dark.

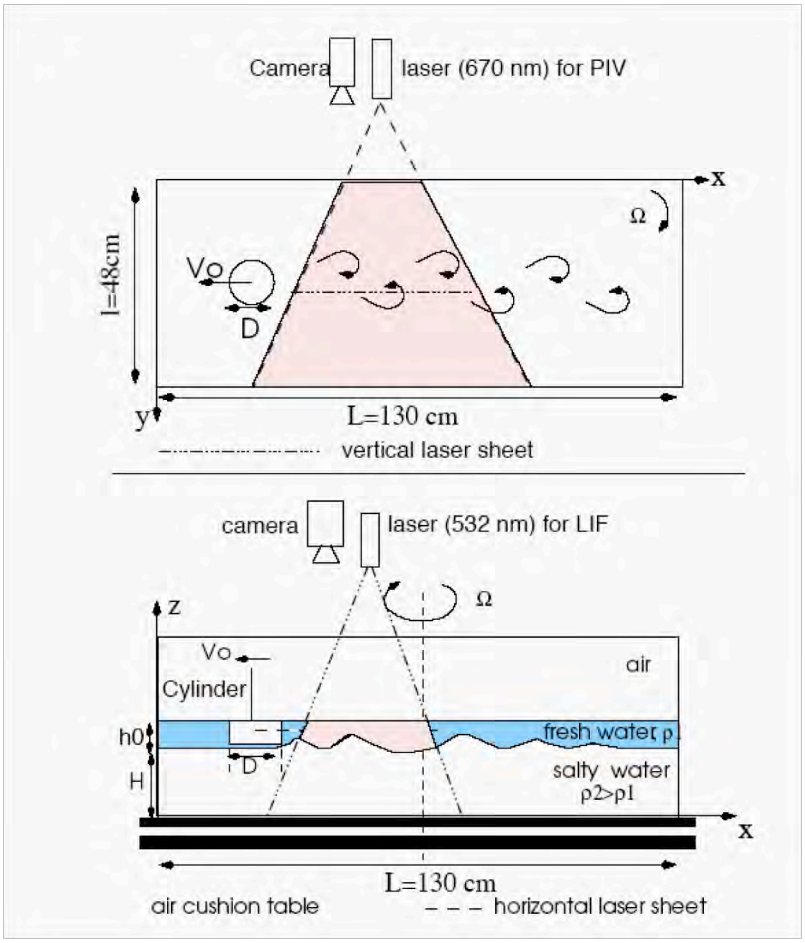

Figure 2: Top and side views of the experiment according to [20]. The fluid is salt stratified in two layers while the cylinder is towed in the thin upper layer. The dynamics are observed and recorded by means of a horizontal and a vertical laser sheet.

3.3 The shallow-water model

To study the stability properties of the upper thermocline layer, we used the reduced gravity rotating shallow-water model on the *f* plane, described in dimensionless form by the following system:

$$\mathrm{Ro}\left(\partial_t \mathbf{V} + (\mathbf{V}.\nabla)\mathbf{V}\right) + f\,\mathbf{n}\times\mathbf{V} = -\frac{\mathrm{Bu}}{\mathrm{Ro}}\nabla\eta + \frac{\mathrm{Ro}}{\mathrm{Re}}\Delta\mathbf{V} \qquad (1)$$

$$\partial_t \eta + \mathbf{V}.\nabla\eta + (1+\eta)\nabla.\mathbf{V} = 0 \qquad (2)$$

with **n** the upward-pointing unit vector, **U** = (u, v) the horizontal velocity scaled by the typical velocity V and η the surface deviation scaled by the unperturbed layer depth h. This single layer rotating shallow-water formulation filters out the three-dimensional perturbations and remain valid if the local vorticity is not too large.

To perform the temporal stability analysis, the shallow water equations are linearized around a mean geostrophic velocity profile. An An approximation of the matrix of the linear operator is computed in a spectral basis with periodic boundray conditions using the standard LAPACK linear algebra package. The nonlinear evolution of the instability is studied by computing the nonlinear evolution of the perturbed parallel flows. The rotating shallow-water equations are discretized in space with a pseudo-spectral method and in time with a second-order Leapfrog scheme.

When computed, the presence of the obstacle is imposed by using a volume penalisation method which considers both the fuid and the solid as the same porous medium, whose permeability tends to zero in the solid domain ., and to infinity in the fuid domain. A Darcy's force term is thus added to the momentum equation, which is solved in the whole domain with periodic boundary conditions. The effect of the penalized terms is similar to no-slip boundary conditions on the island, which results in the formation of boundary layers where vorticity is produced.

3.4 Anticyclonic predominance

For the frontal geostrophic regime, both physical (Figure 3) and numerical (Figure 4) modeling exhibit a significant asymmetry between cyclonic and anticyclonic vortices in the wake. Large-scale anticyclones remain coherent and circular, whereas cyclones tend to be more elongated and distorted. More surprisingly, for the extreme case of strong interface deviation, only an anticyclonic vortex street emerged in the lee of a circular island [20].

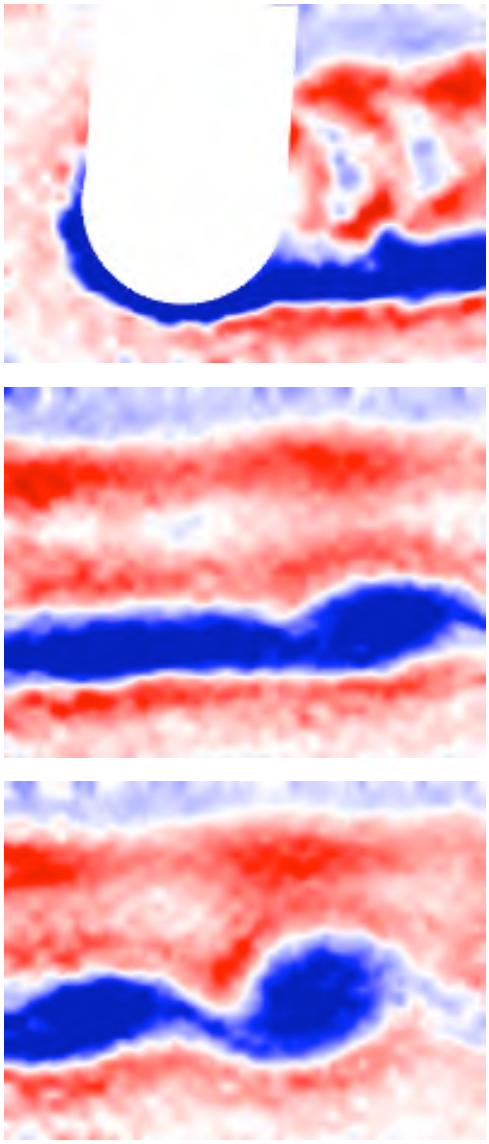

Figure 3: Temporal evolution of the cyclonic (red) and the anticyclonic (blue) vorticity field of a large scale-wake measured by PIV in a rotating shallow-water experiment [20]. The cylindrical island diameter is here significantly larger (D/Rd=6) than the deformation radius (Ro=0.2 and Re=800).

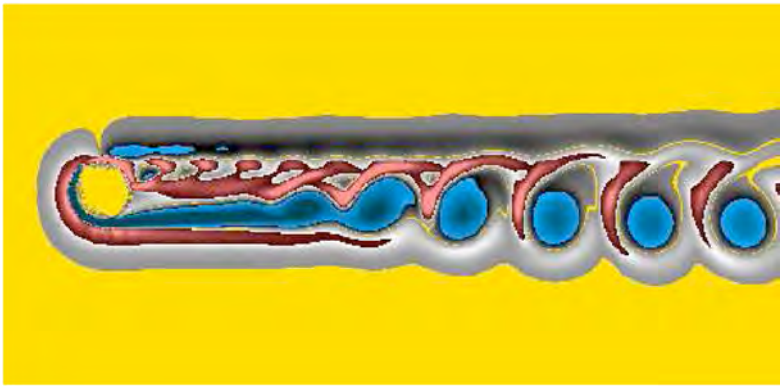

Figure 4: Numerical simulation using a pseudo-spectral scheme with a volume penalization method to reproduce the large-scale wake flow corresponding to the laboratory experiment (Figure.3). Cyclonic (red) and anticyclonic (blue) vorticity.

This cyclone-anticyclone asymmetry of the island wake, may found its origin in the stability properties of parallel shear flows. If we consider the linear stability of an isolated and localized shear flow in a frontal regime [21], the growth rates of the unstable perturbations become significantly higher in the anticyclonic shear than in the cyclonic one (Figure. 5). Hence, if the two lateral shears, which are formed just behind the island in the near wake, are not coupled (it will be indeed the case in the frontal regime, according to 3.6) unstable perturbations will growth faster in the anticyclonic side of the wake leading first to the formation of large-scale anticyclones.

According to the various stability analysis we performed on a wide variety of parallel flows [20, 21], we could emphasize that the barotropic instability of oceanic shears, jets and wake flows favors the formation of large-scale anticyclonic eddies. In the frontal regime (small Rossby number and finite isopycnal displacements), an anticyclonic shear flow will have higher growth rates and be much more unstable than a cyclonic one. The linear stage of the instability induces here a strong cyclone-anticyclone asymmetry and favor the development of unstable perturbations in the anticyclonic shear. The nonlinear saturation leads to the formation of coherent and almost axisymmetric anticyclones, while the cyclones tend to be more elongated in the shear direction once they are formed.

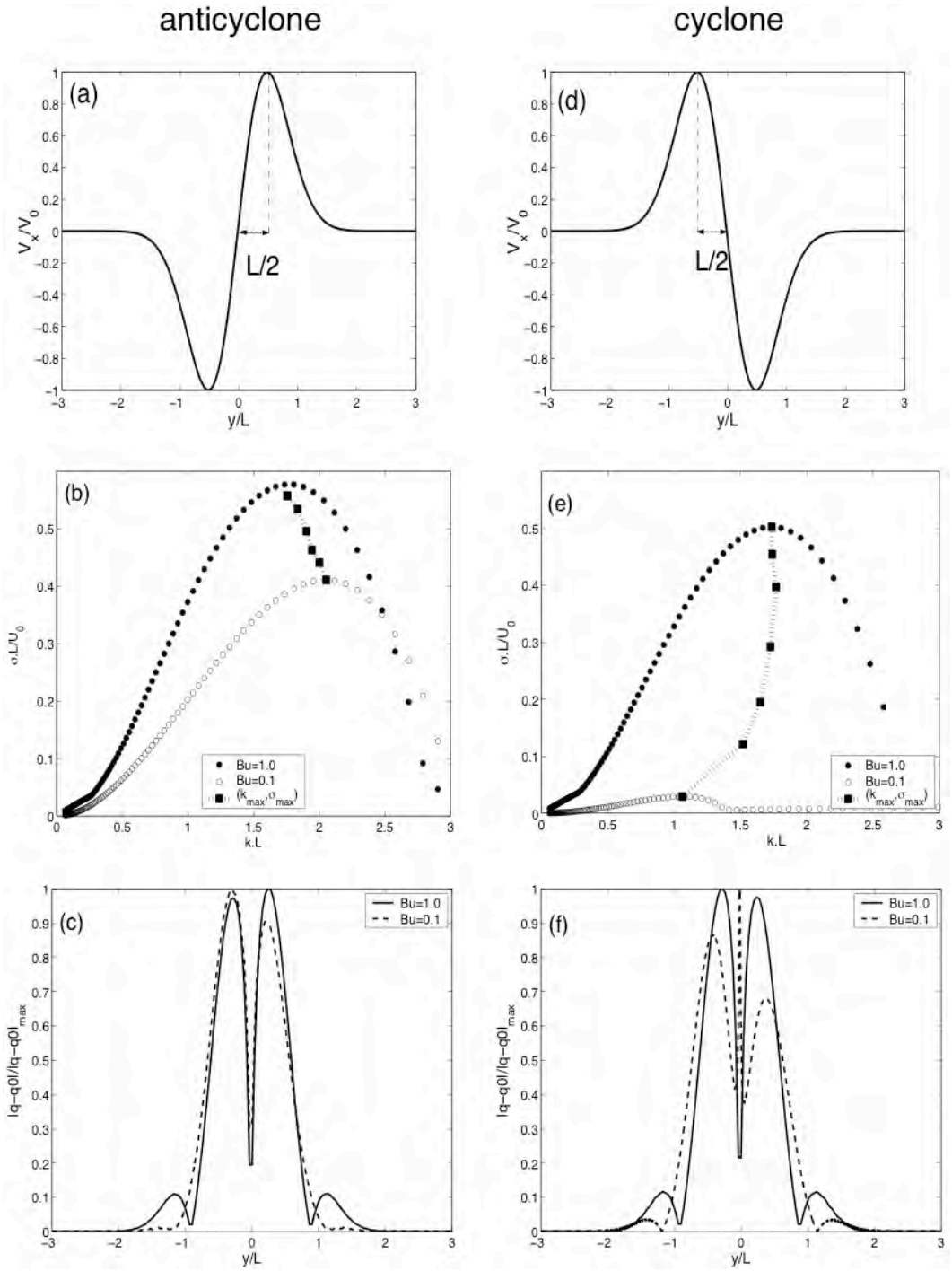

Figure 5: Linear stability of the anticyclonic (a) and the cyclonic (d) localized shear flow for Ro=V_0/fL=0.1 and various Burger numbers [21]. The central panels (b), (e) show the unstable growth rates, calculated both for the quasi-geostrophic (filled dots) and the frontal regime (open dots). The potential vorticity of the most unstable modes are given in the bottom panel (c), (f).

3.5 Increase of the shedding frequency

The main consequence of the distortion or the disappearance of the cyclonic street (Figures 3 and 4) is a strong increase in the Strouhal number. Indeed, the latter can be three times larger than the standard value reached for the same Reynolds number in a classical Karman street (Figure 6). We found that this variation of the Strouhal number and the cyclone-anticyclone asymmetry is governed by a single parameter: the relative

interface deviation λ=Ro/Bu. For small isopycnal deviations the shedding frequency is identical to its classical value in two dimensional flows. The increase of the Strouhal number starts when the surface deviation exceeds 10% of the unperturbed thermocline thickness.

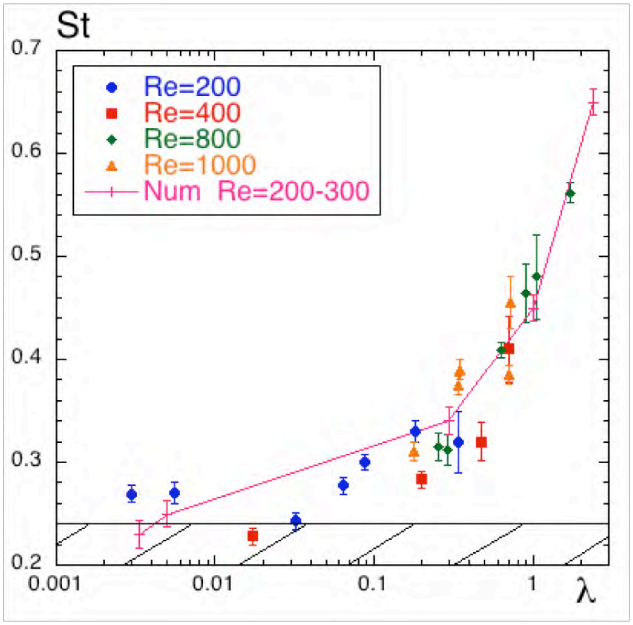

Figure 6: The Strouhal number as a function of the interface deviation parameter for various Reynolds number. Dots correspond to experimental results while crosses to numerical simulation. The dashed zone indicates the range of the Strouhal number for a three-dimensional wake at these Reynolds numbers.

3.6 A convectively unstable wake

Despite its local character, the nonlinear stability analysis, in the frontal regime, recovers the vortex street pattern and the Strouhal number of the laboratory experiment [20]. The similarity between the temporal evolution of the parallel wake and the spatial evolution of real wake suggests that the vortex street formed in the laboratory experiment is due to the noise driven destabilization of the quasiparallel wake extending behind the cylinder rather than the emergence of a global mode as in the classic von Karman street. If so, the instability should be a shear layer-type instability, convective, rather than a wake-type instability, which is absolute in a region of finite extent. To determine a change in nature of the instability, we investigate the absolute or convective character of the present wake instability since this property is believed to determine the global stability of quasiparallel real open flows.

We found that the wake flow measured behind the cylinder is strongly convectively unstable [20]. Since the near wake flow is nearly parallel in the frontal regime [19], this unstable wake would behave like a noise amplifier, the entire flow being convectively unstable. A small wave-packet perturbation is amplified but propagates downstream in the flow and does not contaminate the upstream flow, as it is the case for a quasi-geostrophic wake (Figure 7, upper panel). If the incoming perturbations are small enough, the near wake will looks like a parallel wake flow over a long distance while finite size vortices will emerge only in the far wake (Figure 7, lower panel).

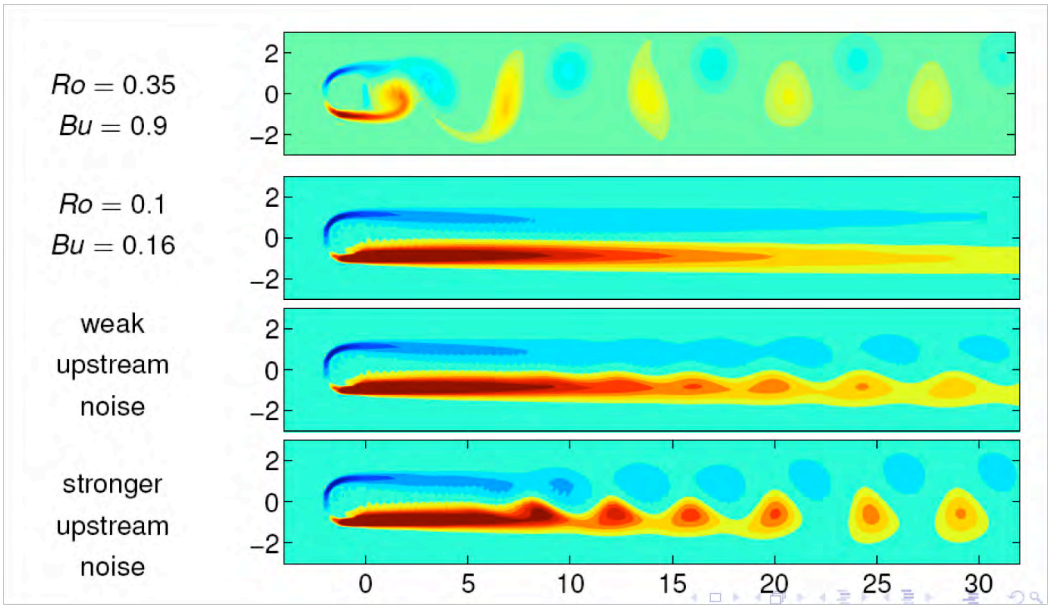

Figure 7: Absolute instability of the wake flow behind a symmetrical island in the quasi-geostrophic regime (upper panel) and the frontal regime (three lower panels) for various amplitude of upstream noise.

For a large scale island (small Burger number), the extend of the double parallel shear in the near wake depends on the amplitude of the incoming perturbations.

4 CYCLOGEOSTROPHIC WAKES

4.1 The cyclogeostrophic regime

When the island or the vortex Rossby number get close to unity (Ro~1) the balance between the velocity and the pressure field is not trivial. Moerover, even for moderate value of the island Rossby number, locally the magnitude of the vorticity could exceed the Coriolis parameter $|\xi| > f$. Such intense vorticity region could be generated by various volcanic islands or archipelago such as Aldabra in the Mozambique channel [22], Cato reef along the Australian coast [23], Agoa-Shima south to the Japanese coast [1] , the Hawaii islands [24], Santa Catalina island [25], or the Gran Canaria archipelago [26]. For these high vorticity values, we cannot construct any asymptotic expansion and balanced models. However, circular and steady vortices will follow the nonlinear cyclogeostrophic balance :

$$\frac{v_\theta^2}{r} + f\, v_\theta = \frac{1}{\rho}\partial_r p \qquad (3)$$

where $v_\theta(r)$ is the orthoradial velocity.

4.2 Experimental configuration

In order to study the impact of rotation and stratification on small-scale instabilities of wake vortices we conducted sixty-seven experiments on the 13-m-diameter rotating platform at the LEGI-Coriolis in Grenoble (France). The turntable had an anti-clockwise rotation (as the planetary rotation) which was kept constant Ω_0=0.069rad.s^{-1} corresponding to a Coriolis parameter f=2Ω_0=0.139rad.s^{-1}. A linear salt stratification was set in the upper layer (h=7cm), which mimic the oceanic thermocline, on the top of a thick barotropic layer (H=50cm) which resembles the deep ocean condition. Strong and weak stratifications were considered corresponding to

Brunt Vaisala frequencies $1<N<3$ s−1. In order to reproduce the dynamic of a surface current interacting with an isolated and steep island (or archipelago) island-like obstacles were towed only in the upper layer. Similar setups are described in Perret *et al.* [20] and Teinturier *et al*. [6]. We assume that the motion of the obstacle transfers momentum mainly in the upper stratified layer and that the dynamic is governed by the first baroclinic mode. This will be generally the case if the lower layer is deep enough, namely when $h<<H$. The towing speed U_0 was varied from 1cm/s to 8cm/s and the corresponding horizontal Reynolds number $Re= U_0D/\nu$ varied from 2500 to 50000, where D is the effective island diameter (D ~ 25-75cm).

The upper layer was seeded with particles of density equal to the mid level of the upper stratification. These buoyant particles were illuminated from bellow with submerged lights. The particles motion were captured by three to four full-frame cameras: two wide-angle cameras captured the global wake dynamics, on zoomed camera follows the evolution of a single eddy and one camera attached to the carriage capture the detached boundary layers (BL) with an high spatial resolution.

4.3 The ROMS model

Small-scale inertial instability were also studied by mean of numerical simulation using the Regional Oceanic Modeling System (ROMS) which solves the rotating primitive equations. It is a split explicit, free-surface oceanic model, where short time steps are used to advance the surface elevation and barotropic momentum equations with a larger time step used for temperature, salinity, and baroclinic momentum (Shchepetkin and McWilliams 2005). A third order, upstream-biased advection operator allows the generation of steep gradients in the solution, enhancing the effective resolution of the solution for a given grid size when the explicit viscosity is small (Shchepetkin and McWilliams 1998). The numerical diffusion implicit in the upstream-biased operator allows the explicit viscosity to be set to be zero without excessive computational noise or instability. An artificial set of boundary conditions is fixed in the vicinity of solid boundaries. These conditions are based on physical considerations that mimic a no-slip rule [5]. They are implemented by an appropriate land-masking rule. As the result, the numerical model “feels” a no-slip boundary even when the explicit eddy viscosity is set to zero because it is always implied that there is an underlying boundary layer with a no-slip condition at the wall.

4.4 Inertial instabilities of circular anticyclones

Inertial and/or elliptical instabilities may strongly destabilize intense anticyclonic eddies [14, 15, 16]. Indeed, three dimensional perturbations growth in a localized region, at the edge of the anticyclonic vortices, if the dimensionless vorticity $\varepsilon=\xi/f<-1$ is negative enough, where ξ is the relative vorticity and $f=2\Omega_0$ the Coriolis parameter. For a columnar vortex, the vertical wavelength of the most unstable mode is mainly controlled by the maximum dimensionless vorticity ε, the Reynolds number Re and the relative stratification parameter N/f [17]. If the incoming oceanic flow is strong enough or if the island diameter is very small, then eddies that will form in the wake will have large vorticity values. In such case, the selective destabilization of anticyclonic eddies, which occurs in a specific range of parameters (Ro, Re, N/f), may favor the emergence of coherent cyclones in the oceanic island wake.

4.5 Cyclonic predominance

The experiments performed on the Coriolis platform have shown that the transient three-dimensional instabilities (inertial,elliptical or centrifugal) do persist in a shallow-water configuration, in other words when the vertical to horizontal aspect ratio is small $\alpha << 1$. By means of dye visualizations, we quantify in the (Ro − Re) parameter space, the specific dispersion regimes induced by the small-scale unstable perturbations [6]. For finite Rossby number (Ro > 0.8) and moderate Reynolds numbers (Re ~ 5000–10 000) the passive dye tracers could be mixed within the core of anticyclonic vortices while for higher Reynolds numbers (Re > 15 000) the passive tracers initially released in the anticyclonic island boundary layer could be strongly stretched and mixed in the near wake flow. On the other hand, in the cyclogeostrophic regime, cyclonic eddies remain coherent and capture a large amount of passive tracer (red dye in Figure 8) in their core. In this specific regime a clear cyclonic predominance occurs.

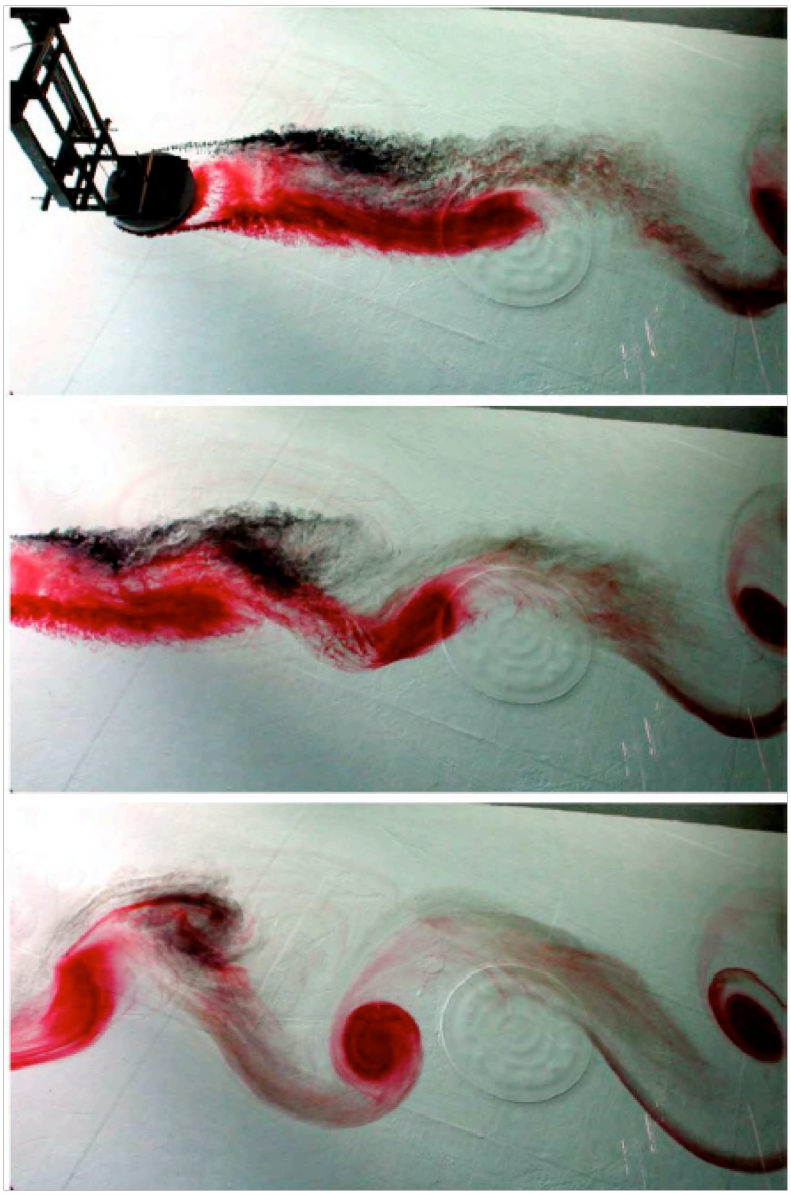

Figure 8: Top-view of dye experiment, for Ro = 2, Re = 20 000, and Bu = 7.5, at (a) t = 0 , (b) t = T_0 T_0, (c) t = $2T_0$ where T_0=30s. The red (black) dye was initially released in the cyclonic (anticyclonic) island boundary layer according to Teinturier *et al*. 2010 [6].

According to qualitative dye visualisation the typical horizontal scale of the unstable disturbances seems to be fixed by the upper layer thickness rather than the size of the unstable region defined by the Rayleigh discriminant. Hence, both the vertical and the horizontal resolution of regional oceanographic models should be increased to capture accurately this small-scale and three-dimensional instability. The increase of enstrophy for higher grid resolution, indicating the emergence of smaller unstable perturbations, was clearly shown by the numerical study of Dong *et al.* [5]. Both numerical simulations and quantitative PIV measurements were performed to study in the cyclogeostrophic regime, the dynamical evolution of the vorticity field in the wake flow.

According to the linear stability analysis of Rankin vortices in a rotating and stratified shallow layer [27], we used four dimensionless parameters which govern the eddy stability, namely: the eddy Rossby number $(Ro)_e$, the vertical Reynolds number $Re=Vh/\nu$, the aspect ratio parameter $\delta=h/R_d$ and the stratification parameter $S=N/f$, where h and N are respectively the thickness and the Brunt-vaisala frequency of the stratified upper layer. For circular vortices, the linearly unstable region is located at the edge of the eddy [17, 6, 27] just after the maximum velocity.

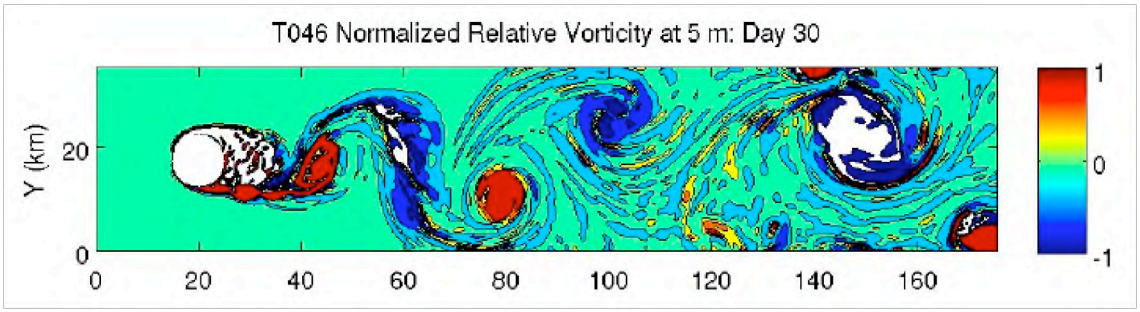

Figure 9: Cyclonic (red) and the anticyclonic (blue) vorticity field for a cyclogeostrophic wake in a linearly stratified thermocline according to ROMS model. The cylindrical island radius is equal here to the deformation radius (Bu=1, Ro=0.8, N/f=10 and Re=6400).

Therefore, if the non-linear evolution is not to strong, the perturbations will weakly affect the core of the eddy. Similar behavior were found from the numerical simulations according to the Figure.9. In such case, unlike the tall column vortices [16] individual anticyclones having large core vorticity values ($\xi/f<-1$) may survive for a long time (Figure 10(b)) due to the combined effect of the stratification ($S>>1$) and the shallow-water constrain ($\delta<<1$). The three dimensional unstable perturbations will then affect mainly the maximum eddy velocity V rather than the core vorticity ξ. A clear asymmetry can be observed between cyclonic (Figure10 (c)) and anticyclonic (Figure 10 (d)) velocity profiles which can be seen as the signature of inertial instability. The stabilizing effect of the stratification is shown in Figure 10 (d) from $S=N/f=7$ to $S=20$.

If the stratification and the shallow water constrain tend to weaken the inertial destabilisation of anticyclones, the most unstable regions of the wake flow will then be the detached anticyclonic boundary layer in the near wake, just behind the islands.

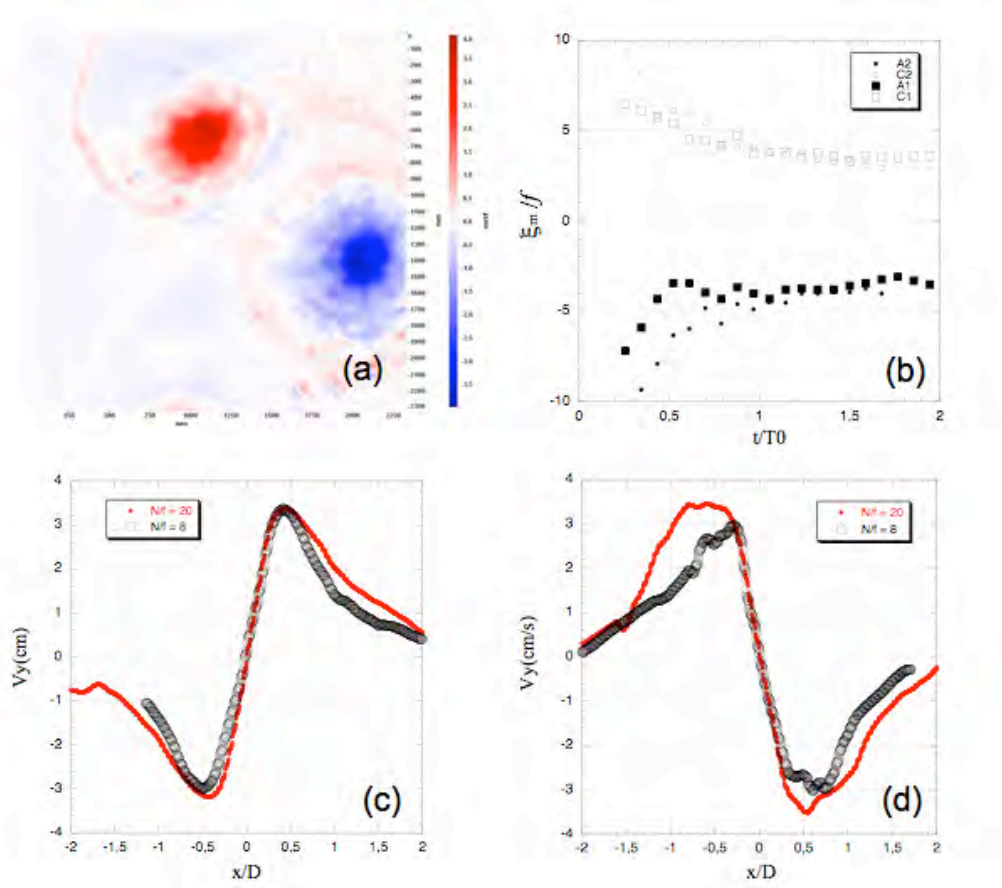

Figure 10 Relative vorticity of cyclonic (red) and anticyclonic (blue) eddies (a); core vorticity evolution (b); cyclonic (c) and anticyclonic (d) velocity profiles corresponding to the parameters: Re~1700, Ro ~ 2, d=0.25 and S= 8 and S=20.

5 ASYMMETRIC ISLAND SHAPE

Another source of asymmetry between opposite sign eddies in the wake could be due to the island shape itself even for a pure two-dimensional flow which is not affected by the rotation and the stratification. For an asymmetrical island the detached boundary layers of the near wake may differ in width and amplitude. In such case, the vortices, which are formed further down in the wake, will differ in size (radius) and intensity (core vorticity).

To study in laboratory the effect of island asymmetry, both symmetric (cylinder & ellipse) and asymmetric obstacles (tilted ellipse and multiple ellipses) were considered with the same stratification and the same incoming current . Preliminary experimental analysis suggests that the pitching of the ellipse enhances (near-field) vortex asymmetry. In the multiple island cases there are also near-field differences (Figure 11 c-d). Whereas in the symmetric cases to the detached boundary layer (Figure 11 a-b) differences are not so apparent, in the tilted and multiple island cases there are strong near-wake instabilities. Multiple islands in the anticyclonic side (Figure 11 c-d) produce independent wakes, which interfere with the anticyclonic shedding. Nevertheless, archipelago/asymmetric cases also induces the formation of coherent vortices (far-field) further leeward, when compared to the symmetric cases, i.e. wider boundary layer width.

It is hypothesized that the contribution of strong positive vortices in the near-field of the anticyclonic side (Figure 11 c-d) as well as the presence of a small nearby island, like the Desertas island in the Madeira Archipelago, might play a significant role. Therefore it is likely that the lack of detection of anticyclones leeward of Madeira is not only caused by the limited remote sensing detection capability but also due to perhaps small near-wake instabilities.

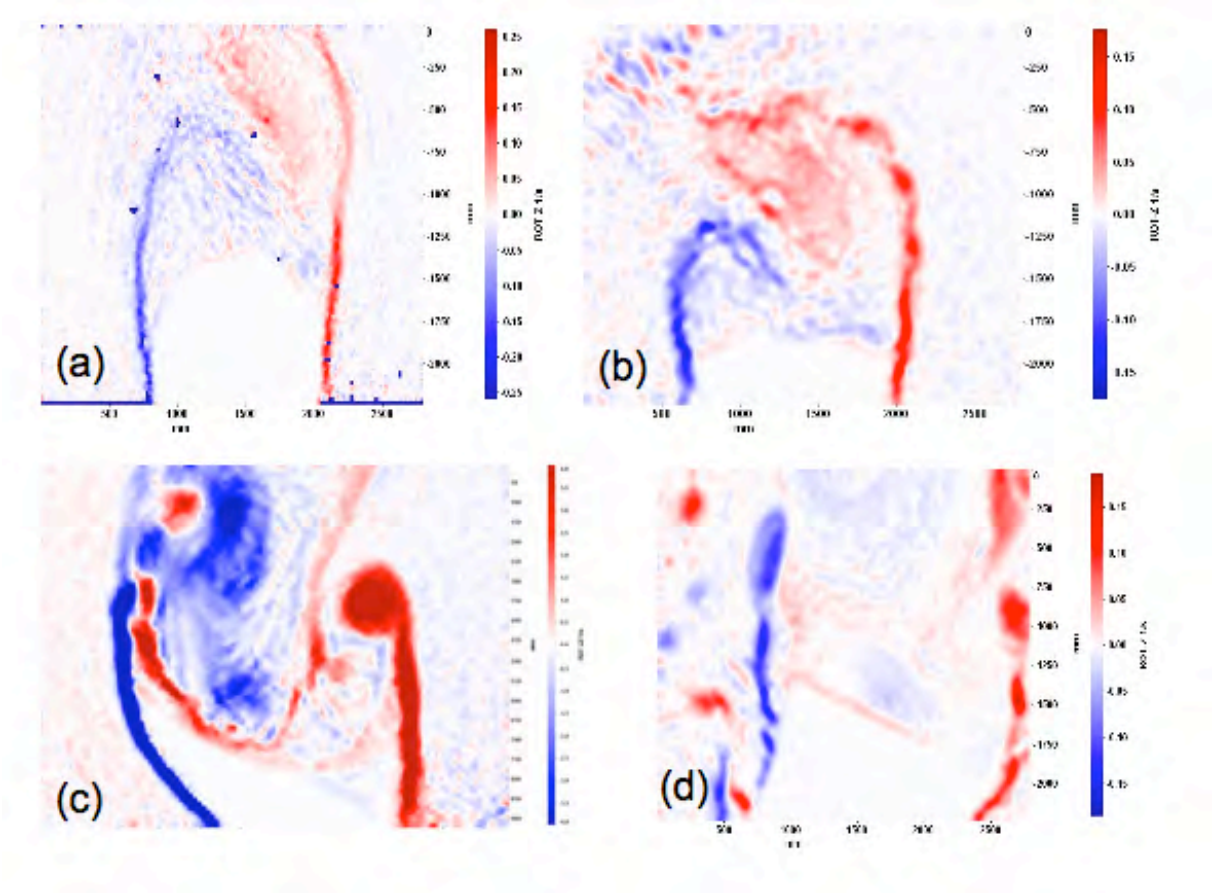

Figure 11 Vorticity field of various boundary layer (near-field) corresponding to different island/archipelago geometries: (a) Cylinder; (b) Ellipse; (c) Two-ellipses; (d) Realistic coastal shape of the Madeira Archipelago.

6 CONCLUSIONS

Both laboratory experiments and numerical simulations exhibit a preferred formation of anticyclonic vortices in the lee of large islands. This asymmetry could find an explanation in the linear stability analysis of frontal wake flows. Then, once they are formed, large-scale anticyclones tend to be more stable and robust to external strain perturbations than their cyclonic counterparts. Hence, if the island or the archipelago is large enough (larger than the deformation radius) we could expect the predominance of large anticyclones in the oceanic wake. Besides, in such case, a transition from absolute to convective instability was also found for rotating shallow-water wakes. The patterns of the convectively unstable wake strongly differ from the standard two-dimensional Karman street and the vortices are shed at an higher frequency.

At smaller scales, ageostrophic filaments and three-dimensional instabilities controls the dynamics. Recent experimental and numerical results have shown that an island wake flow may exhibit a transient and three-dimensional instability in or around the region of intense anticyclonic vorticity. This instability is a branch of the inertial (or centrifugal) instability in the framework of rotating, stratified shallow-water flows. The analysis of the experimental data coupled to high resolution ROMS simulations identify the dynamical conditions (Rossby, Reynolds and stratification numbers) under which the inertial instability affects the wake dynamics and the mixing of passive tracers.

However, not only the size but also the coastal shape of the island and the temporal variability of the oceanic flow could have a strong influence on the eddy formation. For instance, the topography of the Madeira Archipelago favors the formation of large cyclonic eddies in agreement with recent remote sensing observations.

ACKNOWLEDGMENTS

We deeply acknowledge our collaborators: J.M. Chomaz, H. Didelle, T. Dubos, A. Lazar, J. McWilliams, G.Perret, A. Shchepetkin, S. Teinturier, S. Vuiboud for their essential contribution to this work.

An important part of the experimental study has been supported by European Community's Sixth Framework Programme through the grant to the budget of the Integrated Infrastructure Initiative HYDRALAB III within the Transnational Access Activities, Contract no. 022441.

REFERENCES

[1] Hasegawa, D., H. Yamazaki, R. G. Lueck, and L. Seuront, How islands stir and fertilize the upper ocean, Geophys. Res. Lett., 31, L16303, doi:10.1029/2004GL020143 (2004).

[2] Hasegawa, D., M. R. Lewis,1 and A. Gangopadhyay, 2009: How islands cause phytoplankton to bloom in their wakes ? , Geophys. Res. Lett., 36, L20605, doi:10.1029/2009GL039743.

[3] P.Sangra, J.L. Pelegri, A. Hernandez-Guerra, I. Arregui, J.M. Martin, A. Marrero-Diaz, A. Martinez, A.W. Ratsimandresy and A. Rodriquez-Santana, Life of an anticyclonic eddy, J. Geophys. Res., v.110, C03021, dói:10.1029/2004JC002526 (2005).

[4] F. Vidussi, H. Claustre, B. Manca, A. Luchetta and J.C. Marty, Phytoplankton pigment distribution in relation to upper thermocline circulation in the eastern Mediterranean Sea durin winter, J. Geophys. Res., v.106, no C9, p.19939-19956 (2001).

[5] C. Dong, J. McWilliams and A. Shchepetkin, Island wake in deep water, J. Physical Oceanogr. 37, 962-981 (2007).

[6] S.Teinturier, A. Stegner, S. Viboud and H. Didelle, Small-scale instabilities of an island wake flow in a rotating shallow-water layer, Dyn. Atmos. and Ocean, 49, 1-24. doi:10.1016/j.dynatmoce.2008.10.006 (2010).

[7] G.T. Mitchum,The source of 90-day oscillations at wake island. J. Geophys. Res., 100, 2459–2475 (1995).

[8] P.R. Flament, R. Lumpkin, J. Tournadre, and L. Arni, Vortex pairing in an unstable anticyclonic shear flow : discrete subharmonics of one pendulum day. J. Fluid Mech., 440, 401–409 (2001).

[9] L. M. Polvani, J. C. McWilliams, M. A. Spall, and R. Ford, The coherent structures of shallow-water turbulence: Deformation-radius effects, cyclone/anticyclone asymmetry and gravity-wave generation, Chaos 4, 177 (1994).

[10] M. Arai and T. Yamagata, Asymmetric evolution of eddies in rotating shallow water, Chaos 4, 163 (1994).

[11] A. Stegner and D. G. Dritschel, "A numerical investigation of the stability of isolated shallow water vortices," J. Phys. Oceanogr. 30, 2562 (2000).

[12] J.A. Johnson, The stability of shearing motion in a rotating fluid. J. Fluid Mech. 17 (3), 337–352 (1963).

[13] S. Yanase, S., Flores, C., Metais, O., Riley, J.J., Rotating free-shear flows. 1. Linear-stability analysis. Phys. Fluids A-Fluid 5 (11), 2725–2737 (1993).

[14] L.Tarbouriech, L. and D. Renouard, Stabilisation et destabilization par la rotation d'un sillage turbulent, C. R. Acad. Sci. III 323, 391 (1996).

[15] D. Ya. Afanasyev, Experiments on instability of columnar vortex pairs in rotating fluid, Geophys. Astrophys. Fluid Dyn. 96,31 (2002).

[16] A. Stegner, A., T. Pichon and M. Beunier, Elliptical-inertial instability of rotating Karman vortex streets, Physics of Fluids, 17, 066602 (2005).

[17] R.C. Kloosterziel, Carnevale, G.F., Orlandi, P., Inertial instability in rotating and stratified fluids: barotropic vortices. J. Fluid Mech. 583, 379–412 (2007).

[18] M. Tomczak, 1988. Island wakes in deep and shallow water. J. Geophys. Res. 93, 5153–5154.

[19] B. Cushman-Roisin, Frontal geostrophic dynamics, J. Phys. Oceanogr. v.16, 132 (1986).

[20] G. Perret , A. Stegner, M. Farge, T. Pichon, Cyclone-anticyclone asymmetry of large-scale wakes in the laboratory. Phys. Fluids, 18 (2006).

[21] G. Perret , T.Dubos, A. Stegner, How large scale and cyclogeostrophic barotropic instabilities favor the formation of anticyclonic vortices in the ocean. *Submitted to*

J.Phys. Oceanogr, (2010).

[22] Heywood, K.J., Stevens, D.P., Bigg, G.R.. Eddy formation behind the tropical island of aldabra. Deep-Sea Res. Pt. I 43 (4), 555–578 (1996).

[23] Coutis, P.F., Middleton, J.H. Flow-topography interaction in the vicinity of an isolated, deep ocean island. Deep-Sea Res. Pt. I 46 (9), 1633–1652 (1999).

[24] Chavanne, C.,. Observations of vortices and vortex rossby waves in the lee of an island. In: Proceeding, CFM Grenoble (2007).

[25] Caldeira, R.M.A., Marchesiello, P., Nezlin, N.P., DiGiacomo, P.M., McWilliams, J.C.,. Island wakes in the southern California bight. J. Geophys. Res., 110 (2005).

[26] Aristegui, J., Sangra, P., Hernandezleon, S., Canton, M., Hernandezguerra, A. Island-induced eddies in the canary-islands. Deep-Sea Res. Pt. I 41 (10), 1509–1525 (1994).

[27] A.Lazar, A. Stegner, H. Eifetz, Inertial instability of surface vortices in the laboratory and the ocean, Part I: linear stability analysis. *in preparation.*